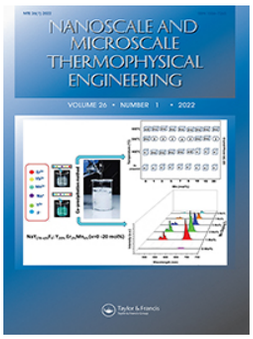

Taylor & Francis
Taylor & Francis Group

Nanoscale and Microscale Thermophysical Engineering

ISSN: (Print) (Online) Journal homepage: https://www.tandfonline.com/loi/umte20

Thermal Protection Performances of the Macro and/or Nano Enhanced PCM in a Representative Battery Pack

Umit Nazli Temel, Ferhat Kilinc & Serkan Coskun

To cite this article: Umit Nazli Temel, Ferhat Kilinc & Serkan Coskun (2022) Thermal Protection Performances of the Macro and/or Nano Enhanced PCM in a Representative Battery Pack, Nanoscale and Microscale Thermophysical Engineering, 26:1, 52-66, DOI: 10.1080/15567265.2022.2069615

To link to this article: https://doi.org/10.1080/15567265.2022.2069615

Published online: 27 Apr 2022.

Submit your article to this journal

Article views: 248

View related articles

View Crossmark data

Citing articles: 1 View citing articles

Full Terms & Conditions of access and use can be found at
https://www.tandfonline.com/action/journalInformation?journalCode=umte20

NANOSCALE AND MICROSCALE THERMOPHYSICAL ENGINEERING
2022, VOL. 26, NO. 1, 52–66
https://doi.org/10.1080/15567265.2022.2069615

Taylor & Francis
Taylor & Francis Group

Check for updates

Thermal Protection Performances of the Macro and/or Nano Enhanced PCM in a Representative Battery Pack

Umit Nazli Temel [a], Ferhat Kilinc [a], and Serkan Coskun [b]

[a]Department of Mechanical Engineering, Sivas Cumhuriyet University, Sivas, Turkey; [b]Department of Energy Systems Engineering, Sivas Cumhuriyet University, Sivas, Turkey

ABSTRACT

This experimental study focused on the comparison of thermal protection performances of macro and/or nano enhanced organic PCM in a representative battery pack from low to high discharge rates. The macro/nano enhanced RT-44 provides the desired battery thermal protection requirements in terms of criteria such as maximum temperature and maximum temperature difference restriction and uniform temperature distribution throughout the battery pack. It increases the effective battery thermal protection time by 117%-32% depending on the discharge rates. While PCM thermal protection provides a more homogeneous temperature distribution throughout the battery pack, nano and/or macro enhanced one provides it throughout the cell. The macro enhancement essentially makes a major contribution to shortening the cooling time for the next use.

ARTICLE HISTORY
Received 12 November 2021
Accepted 18 April 2022

KEYWORDS
Battery pack; passive thermal protection; PCM; graphene nanoplatelets

1. Introduction

Li-ion batteries stand out as primary power sources for electric vehicles due to their superior advantages such as high specific power, high specific energy density, long cycle life, low self-discharge rate, and high discharge voltage [1, 2]. However, li-ion cells are exposed to heat generation during operation, depending on their inner resistance and chemical reaction. Notably, the high discharge current results in a high heat generation rate and a rapid temperature rise on the battery [3, 4]. It may lead to some disadvantages such as thermal imbalance, capacity and performance loss, and severe security problems like thermal runaway and explosion [5]. Ramadass et al [6]. investigated the capacity fades of 18650 (1.8Ah) li-ion batteries operating at different temperatures for a large number of charge/discharge cycles. The capacity fades of the cells at the operating temperatures of 25°C and 45°C at the end of 800 charge/discharge cycles were determined as 31% and 36%, respectively. On the other hand, they determined that Li-ion batteries operating at 50°C lost 60% of their capacity at the end of 600 charge/discharge cycles. To overcome these disadvantages, the use of an effective thermal protection system is necessary. It is also desirable to have a temperature distribution of <5°C from module to module [7]. Regarding the above results, an effective thermal protection system should keep the maximum temperature and temperature difference inside the package below 50°C and 5°C, respectively

One of the thermal protection methods of li-ion batteries is passive thermal management based on PCM usage. This process is based on absorption/release of the latent heat during the phase change of PCM [8]. The PCM with high latent heat can reduce the peak temperature and the temperature difference during the battery operation [9, 10]. Solid-liquid PCM was mostly preferred in the previous studies due to the little volume change during the phase change [11]. Paraffin is a solid-liquid PCM with a significant energy storage capacity that can be used for battery thermal protection. It has several

CONTACT Umit Nazli Temel untemel@cumhuriyet.edu.tr Department of Mechanical Engineering, Sivas Cumhuriyet University, 58140 Sivas, Turkey

© 2022 Taylor & Francis

evident advantages: high stability, low cost, and nontoxic and non-corrosive effects. The paraffin-based PCMs suffer from low thermal conductivity and cannot provide proper thermal protection to the battery during a long operation with high discharge rates [11, 12]. This is because the amount of heat penetration and the contact temperature of the battery are the functions of PCM thermal conductivity [13]. While heat penetration varies in direct proportion to PCM thermal conductivity, battery contact temperature varies inversely. So, they are ineffective in heat dissipation for li-ion battery protection, and they may cause thermal runaway and even explosion [14]. Therefore, the thermal conductivity of PCMs to be used in battery thermal protection should be improved first.

The combination of the PCM with fins was the first method that comes to mind for using thermally enhanced PCM in the battery thermal protection. Ping et al. [15] investigated the effects of fin thickness, fin spacing and PCM thickness on the thermal performance of battery modules. They reported that the fin thickness of 0.5 mm, the fin spacing of 2.5 mm and the PCM thickness of 10 mm are the optimum conditions in terms of reducing the maximum cell temperature and maintaining a more uniform temperature throughout the package. Wang et al. [16] performed an experimental performance study of a battery pack containing cylindrical cells using PCM with thermally enhanced metal fins. However, the use of metal fins together with the PCM causes an undesirable increase in system weight and volume.

The PCM impregnated foam is another technique used for the effective thermal protection of battery packs. In this respect, it has been determined that aluminum [17, 18] and copper foam/PCM [19, 20] composites reduce the battery cells' maximum temperature by 50%. In the last decade, expanded graphite/PCM composites have been widely used for battery thermal management due to low weight, high resistance to corrosion and ease of use [21]. Additionally, the leakage problem of liquid PCM is prevented by the strong capillary force provided by the expanded graphite (EG) matrix [22]. Xu et al. [23] examined the thermal protection of cells in a cylinder package with EG/paraffin composite in terms of the composite density and paraffin fractions. They recommended that the 75% paraffin/EG composite with a density of 890 kg/m^3 for battery thermal management. Jiang et al. [24] proved that EG/Paraffin composites significantly reduce battery cells' temperature rising while keeping the maximum temperature difference around 1–2°C within the battery pack. The major disadvantage of this method is the limited amount of PCM to be impregnated into the foam pores.

Another method used to improve their low thermal conductivity is to incorporate nanoparticles with high thermal conductivity within the PCM. Carbon-based nanoparticles have been reported to effectively enhance the thermal conductivities of PCM compared to metal/metal oxide nanoparticles [25]. Additionally, the shape of the nanoparticles also affects this enhancement and the planar-shaped nanoparticles were found to be more successful in this respect [26–28]. Graphene nano-platelets (GNP) are planar-shaped and suitable nanoparticles that can be used to enhance PCM thermal conductivity [29]. Goli et al. [30] showed that the thermal management of li-ion cells in a cylindrical package can be drastically improved using PCM with Graphene nano fillers. They reported that the improved heat conduction toward the outside significantly lowered the temperature inside the li-ion battery package. Temel et al. [31] reported that the 7% Graphene nanoplatelets incorporation increased the effective passive thermal protection duration by 2 times compared to PCM in a simulative battery pack.

Several hybrid hybrid methods have also been tested for PCM based battery thermal protection. Ling et al. [32] tested the hybrid thermal protection system consisting of PCM and forced convection on 5S4P (five cells in series and four cells in parallel) li-ion cells in a rectangular package. They determined that the combined system prevents the heat accumulation and keeps the maximum temperature of the pack under 50°C. Kong et al. [33] proposed a coupled composite phase change material and liquid cooling for the thermal protection of lithium-ion battery pack. They reported that the coupled system exhibited good thermal protection at an ambient temperature of 30°C such that it kept the maximum temperature and temperature difference of the battery pack at 41.1°C and 4°C at the end of 3C discharge. Youfu et al. [34] proposed low density polyethylene to prevent leakage problem of paraffin and expanded graphite-fin combination to improve the thermal conductivity of

paraffin to be used in battery thermal protection. They found that constructed PCM-based battery module presents excellent heat dissipation performance, allowing the battery pack to operate with the safety temperature of 50°C and temperature difference of 5°C.

This study focused on the comparison of thermal protection performances of macro, nano and hybrid (macro/nano) enhanced PCM in a representative battery pack. The macro enhancement was carried out by adding copper shavings particles into the PCM as a simple but untested method in the literature. The nano enhancement was achieved by adding planar-shaped and carbon-based nano-particles into PCM. To investigate the combined effect of macro and nano enhancement, a macro/nano enhanced PCM composite was also created. Performance evaluations of PCM-based passive thermal protections with different enhancement methods were performed in a representative battery pack from low to high discharge rates.

2. Experimental methods

RT-44 (Rubitherm Technologies, Germany) is a paraffin-based organic PCM used in this study with a suitable melting temperature range (41–44°C) for the thermal protection of battery packs. The helical copper metal shavings with a thickness of 0.2 mm, a width of 4 mm, and a length of 100 – 200 mm were used as supporting material for macro enhancement (Figure 1). The GNP nanoparticles (GNP, Skyspring Nanomaterials Inc, USA), used as supporting material for nano enhancement, have a surface area of 150 m^2/g and a thickness of 6–8 nm (Figure 1).

The nano enhanced composites (GNP/RT-44) were prepared by adding 7% GNP by mass into completely molten RT-44 on a hot plate. The melt mixture was subjected to an ultrasonic mixing for 30 minutes to obtain a homogeneous dispersion. It has been recognized that the addition of 7% GNP is a mixable upper limit in the molten RT-44. Thermal conductivity, DSC, and viscosity characterization of the RT-44 and GNP/RT-44 composites were carried out using KD2 Pro (Jeiotech, South Korea) and DSC-60 (Shimadzu Corporation, Japan) and rotary rheometer (Malvern Kinexus PRO, Switzerland) devices, respectively.

In this study, li-ion battery packs were created representatively using cylindrical electrical heaters instead of real cells. The dimensions of the heaters were adjusted to be similar to the genuine 18,650 (18 mm in diameter and 65 mm in height) li-ion cell. The battery packs were obtained by mounting equally spaced electrical heaters vertically in a rectangular aluminum container. The particular geometric properties of the battery pack were given schematically in Figure 2. Molten RT-44 or nano enhanced RT-44 (7% GNP/RT-44) was poured directly into the battery pack. Then the battery packs were expected to solidify at room temperature, and the heater cells were wrapped in RT-44 (or GNP/RT-44). The macro enhanced RT-44 or macro/nano enhanced RT-44 (macro enhanced 7% GNP/RT-44) to be tested in battery pack thermal protection was prepared by the following method. Firstly, 20% by mass copper shavings were placed around the cells to form a metal mesh structure within the package (Figure 2). Then, the molten RT-44 or 7% GNP/RT-44 was poured into the battery

Figure 1. Macro and nano supported material for the enhancement.

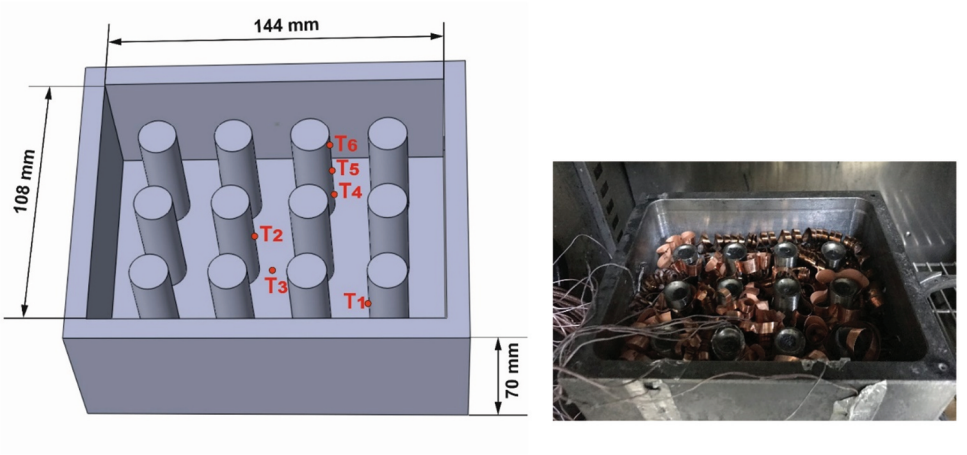

Figure 2. The representative battery pack and temperature measuring points.

pack surrounding both the cells and the copper shaving mesh to be solidified at room temperature. The center-to-center distance between the two adjacent heaters was fixed at approximately 36 mm so that the optimum RT-44 (or GNP/RT-44) thickness of 9 mm was set for each heater [17]. A high temperature resistant gasket was used between the heater and container connection areas to solve the sealing problem.

The experimental rig used in the experiments consists of battery pack, DC power supply, thermocouple connections, data collector, KD2 Pro (thermal conductivity measurement device) computer, and an air conditioning unit (Figure 3). The J-type thermocouples measured time-dependent temperature at specified points in the battery packs. All thermocouples were mounted on the half depth of the heater and named as shown in Figure 2. At the same time, two additional thermocouples (T_4 and T_6) were connected to the lower and upper regions of a specific heater additionally to examine temperature variation across the heater height.

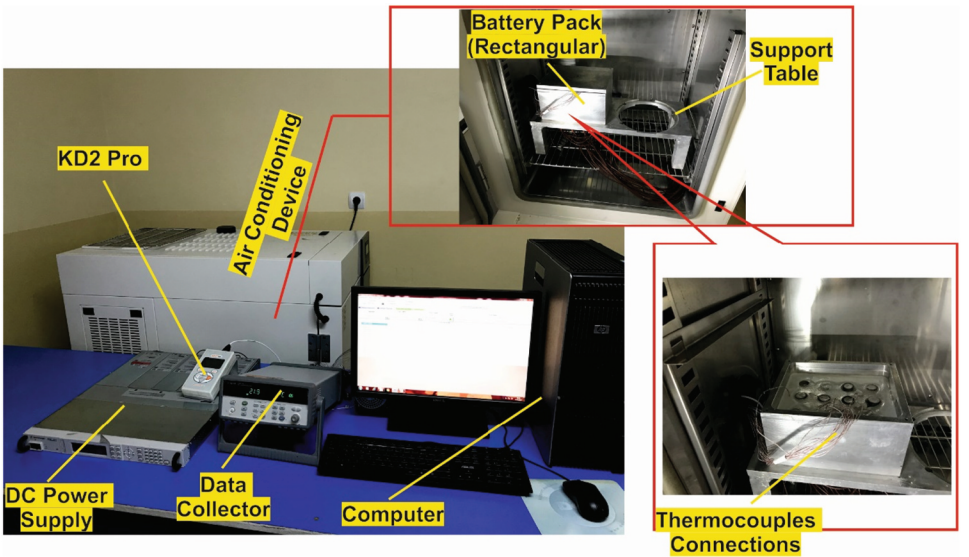

Figure 3. Experimental test rig.

The J-type thermocouples with an accuracy of ± 0.5°C have gathered temperature data at 30 second intervals via a data collector (Agilent 34970A) and transferred it to a computer. In practice, the amount of heat dissipation of a li-ion battery is a function of state of charge, rate of discharge and the operating temperature. The increase in discharge rate is directly related to the amount of heat dissipated. This was achieved by increasing the resistance power in this study. The state of charge and operating temperature of the li-ion battery also affects the dissipation heat during the operation. The effects of the state of charge and operating temperature on the dissipating heat of Li-ion battery were not considered in this study. Battery cells were assumed to be unaffected by the state of charge and the operating temperature, and therefore it emits constant heat. The state of charge and operation temperature effects are left as the subject of a future study. As a representative battery cell, the heaters were assumed to emit constant heat during the discharge process. Each heater was connected to a DC power supply to emit 2.2 W, 4.4 W, 6.6 W, and 8.8 W, respectively. Thereby, different discharge rate scenarios were created for the representative battery pack. The representative battery pack tested for different protection systems in an air-conditioning cabinet maintained a constant temperature of 20°C. Natural convection measurements were also carried out by running the battery pack empty under the same conditions. Natural convection state is sometimes referred to as a thermally unprotected system.

The thermal conductivity measurements were performed by using a KD2 Pro device (Decagon Devices Inc, USA) at 20°C for the solid phase in an air conditioning device. It works based on the transient linear heat source principle. Measuring the temperatures during the heating period, the sensor of the KD2 Pro operates both as a heater and a temperature sensor. The thermal conductivity value is determined by analyzing the measured temperatures over time. The accuracy of the KD2 Pro was ±0.02 W/mK, at least five measurements were made for each sample by recording the mean values with a standard deviation of 0.5.

The Differential Scanning Calorimetry (DSC) properties (melting temperature and melting latent heat) were measured by using Differential Scanning Calorimetry (DSC-60 Shimadzu, Japan). The ramp rate of the device was adjusted to 2°C/min between the temperature range of 20°C and 60°C. The accuracy of DSC was 0.1°C, at least three measurements were made for each sample and mean values were recorded with a standard deviation of 1%.

3. Results and discussions

The effect of macro and/or nano enhancement on the thermophysical properties such as thermal conductivity, melting temperatures, latent heat, and dynamic viscosity have been reported in this section. The thermal conductivity values of macro and/or nano enhanced RT-44 were given in Figure 4. The applied macro enhancement causes an increase of 1.97 times in thermal conductivity while the nano enhancement causes an increase of 3.3 times. The synergistic effect of the macro and nano thermal conductivity enhancement was measured to be 4.2 times, a relatively lower enhancement compared to the sum of the independent effects. This is based on a non-linear character of the thermal conductivity increase.

DSC analyses were conducted to investigate the effect of macro and nano additives on the thermal properties such as melting onset temperature (T_{om}), melting endset temperature (T_{em}) and melting latent heat (H_m). Figure 5 depicts DSC curves of the macro and/or nano enhanced RT-44 composites. It is seen that macro enhancement causes significant changes in DSC curves compared to nano enhancement. The quantitative results for the melting temperatures and latent heats of macro and/or nano enhanced composites were calculated by the DSC software and were compared in Table 1. The melting onset (T_{om}) and melting endset temperatures (T_{em}) remained unaffected by the nano enhancement. On the other hand, it is clear that the macro enhancement causes decrease in the related temperatures. For example, while the melting onset temperature (T_{om}) for RT-44 is 40.22°C, it decreases to 36.9°C when it comes to macro/nano enhanced RT-44. This variation can be attributed to the heat transfer rate and the solid/PCM interface. Similarly, the reduction in the latent heat is also

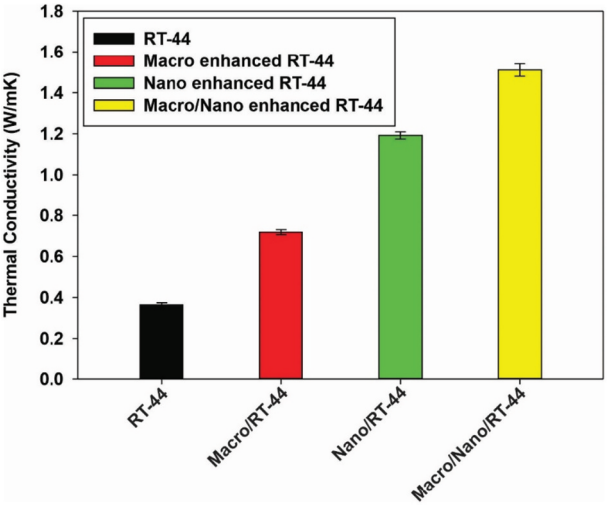

Figure 4. Thermal conductivity values of macro and/or nano enhanced RT-44.

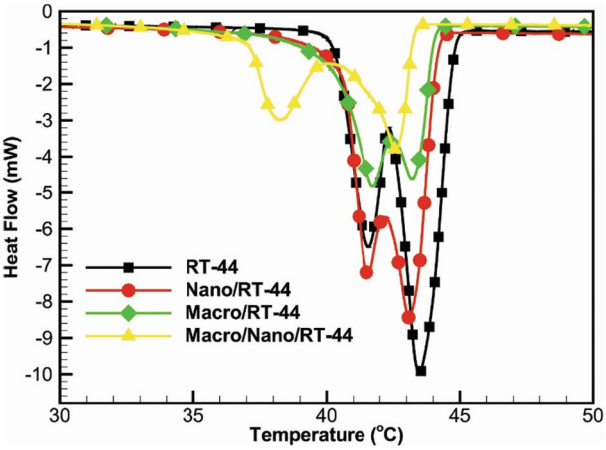

Figure 5. DSC curves of the macro and/or nano enhanced RT-44 composites.

Table 1. The thermophysical properties.

Material	T_{om} (°c)	T_{em} (°c)	H_m (J/g)	$\mu_{@50^\circ C}$ (kg/ms)
RT-44	40.22	44.70	239.6	0.0082
Macro enhanced RT-44	39.28	43.98	167.5	-
Nano/RT-44	40.29	44.92	221.5	0.033
Macro/Nano enhanced RT-44	36.89	43.26	152.8	-

affected by the macro enhancement. For example, while the latent heat (H_m) was decreased by 7.5% in nano/RT-44 composite, decreases of 30.1% and 36.3% were detected in macro/RT-44 and macro/nano/RT-44 composites, respectively. Macro and nano additives can be said to have negative effects on dynamic viscosity as well as melting latent heats. Four times increase in dynamic viscosity (μ) occurs only with the addition of 7.5% nanoparticles Although the capacity loss in the latent heat is tolerable, an increase in the dynamic viscosity causes significant effects on the heat transfer mechanism especially in the liquid phase.

Firstly, the heat powers of the electric heater were correlated to the real li-ion cell discharge rates. Hémery et al. [35] matched the temperature rise of a real li-ion battery operating at 0.5C, 1C, 2C, 3C discharge rates with electrical heater powers. In their study, the temperatures were measured both on the wall of a Li-ion cell and at the cylinder axis, and the corresponding heater powers were averaged. The data obtained were plotted in Figure 6 and an appropriate curve was fitted. The heater powers used in this study were determined by using a specific curve equation (Table 2).

The thermal protection performances of macro and/or nano enhanced RT-44 were compared in terms of battery pack maximum temperature, maximum temperature difference and effective protection times. Undesired heat accumulation causes the cells in the central area of the battery pack to reach the maximum temperature. In the experiment, the maximum temperature was measured at point #T_2 and is given in Figure 7 versus time. It demonstrates a period longer than the battery cell discharge time to make some observations.

The maximum temperature curves of the unprotected (natural convection) battery pack undergo a parabolic increase toward a limit value with the establishment of thermal equilibrium after an initial rapid increase. These parabolic increase rates are proportional to the discharge rates and the maximum temperatures exceed the critical temperature of 45°C in a short period of time at all discharge rates. However, RT-44 based thermal protection significantly restricts the maximum temperature of the battery pack at all discharge rates. Since melting has not yet started, RT-44 exhibits similar but lower maximum temperature responses to natural convection only at low discharge rate (2.7C). In contrast, the maximum temperature curves present the behavior of different regimes at high discharge rates where phase change occurs.Firstly, the maximum temperature of the battery pack rises quickly before the melting process of RT-44. At this regime, heat transfer takes place entirely by conduction and the maximum temperature of the battery pack is significantly reduced due to more heat penetration to the RT-44 compared to natural convection. The restriction of the maximum temperature is an essential protection performance for the battery packs, but it decreases as the discharge rate increases. Further reduction of the slopes of the curves in the second regime formed with the onset of melting is

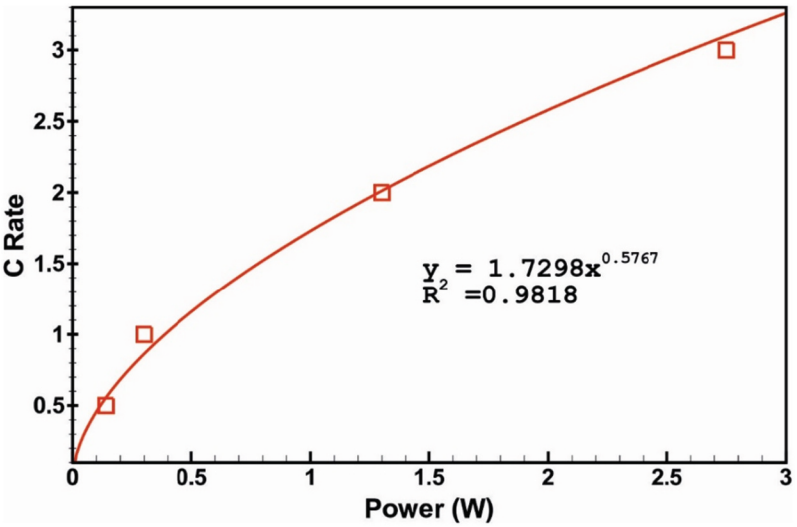

Figure 6. Discharge rates corresponding to heater powers.

Table 2. Discharge rates corresponding to heater powers (this study).

Power(W)	2.2	4.4	6.6	8.8
C Rate	2.7	4.0	5.1	6.0

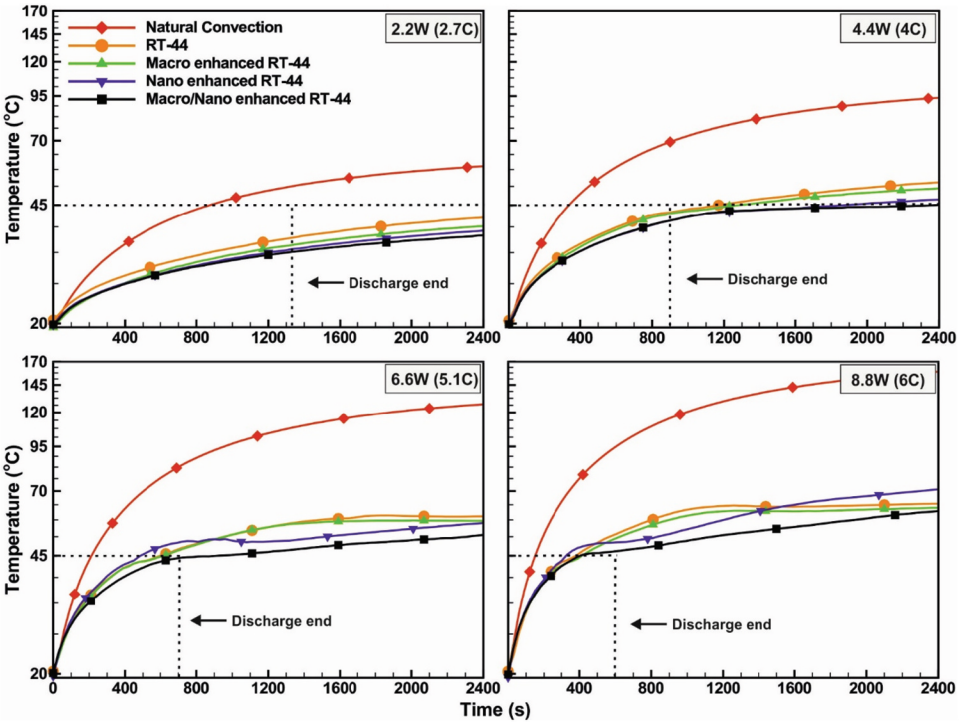

Figure 7. The variation of the maximum temperature of the battery pack with time.

important in terms of limiting the maximum temperature. With liquefying of the mushy zone around the cells, the effective heat transfer mechanism turns from conduction dominant to convection at the second regime. Also, the second regime shortens and its slope increases depending on the discharge rate magnitude. When the liquid around the cells reaches a certain thickness, the convective heat transfer mechanism becomes dominant under the effect of significant buoyancy forces near the cells. In this third regime, the battery maximum temperatures remain nearly stable throughout constant temperature plateaus. However, aforementioned constant temperature plateaus occur at a high temperature and in a short time due to increased discharge rates. The constant temperature values were measured at approximately 53.5°C, 58.5°C and 62.1°C for the discharge rates of 4C, 5.1C and 6C respectively. Especially at high discharge rates, it may be advantageous to reduce the constant temperature plateaus below 45°C, the critical temperature for battery pack thermal protection.In this respect, macro and/or nano enhancements were carried out on the PCM to reduce the constant temperature plateau to lower temperatures. The maximum temperature curves were seen to behave in the exact same way with the macro enhanced RT-44. However, it can be said that copper shaves create a network structure that will help to transmit the heat released from the cells to the inner RT-44 regions. As a result, the maximum temperature values tend to have lower values. The maximum temperature curves of the nano enhanced RT-44 present some distinct differences. Since the thermal conductivity coefficient is enhanced at 7% GNP/RT-44, the maximum temperatures of the battery pack are better restricted in the conduction dominated regimes especially at lower discharge rates (<4C). At high discharge rates (>4C), it is an advantage that the mushy region quickly liquefies with enhanced thermal conductivity and the constant temperature plateau occurs at a lower temperature (≈50°C). However, considering the cell discharge time, reducing the aforementioned constant temperature plateau below 45°C is essential for an effective protection. This enhancement is partially achieved by macro/nano enhanced RT-44. On the contrary, the short duration of the mentioned constant temperature plateau is an important disadvantage. This is because the convective flows that

started in the narrow liquid region around the battery cells are slowed down due to the higher viscosity of 7% GNP/RT-44 as the liquid region begins to expand. At this regime under a weaker convection heat transfer mechanism, the maximum temperature curves start to increase again. As a result, it underperforms the RT-44 after a breakeven point (t = 2845 s for 5.1C and 1490 s for 6C). Fortunately, this only happens after the cell has been fully discharged.

The restriction of the maximum temperature of the battery pack is an important performance criterion for the thermal protection of the battery pack. The maximum temperatures at the end of the discharge and the related percentage performance enhancements in comparison to RT-44 were given in Figure 8 for the macro and/or nano enhanced RT-44. The maximum temperatures of the battery pack were measured to be 51.3°C (2.7C), 69.4°C (4C), 82.8°C (5.1C) and 94.6°C (6C) in the natural convection cases as shown in Figure 8. In other words, the maximum battery pack temperature exceeds 45°C at all discharge rates and therefore it requires the use of thermal protection. With RT-44, the maximum battery pack temperatures were restricted significantly to the values of 35.9°C (2.7C), 42.8°C (4C), 47.2°C (5.1C) and 52.0°C (6C), and performance enhancements were achieved in the range of 30%-45% compared to the unprotected battery pack. However, RT-44 protection provides the ideal protection at 2.7C and 4C while remaining insufficient at 5.1C and 6C. Macro and/or nano enhancements on the RT-44 have resulted in a better and improved protection performance. The macro and/or nano enhanced composites provide an additional several degrees of restriction for maximum temperatures compared to base materials. For instance, at the discharge rates of 2.7C and 4C, the macro or nano enhanced composite provides an approximate 6–9% performance increase compared to the RT-44 and keeps the battery maximum temperatures safe below 45°C. On the other hand, both macro enhanced or nano enhanced RT-44 do not provide ideal protection at high discharge rates (>5.1C). The maximum battery pack temperatures for macro or nano enhanced RT-44 exceed 45°C, so they provide only effective protection for a limited time at the discharge rate of 5.1C and 6C. Moreover, the nano enhanced RT-44 performs worse at 5.1C discharge rate in terms of maximum temperature restriction. The reason for this is that the heat conduction is less than RT-44 until convective currents start in the liquid layer, which is formed quickly due to the increased thermal conductivity in nano enhanced RT-44. Because of the molecular disorder, the thermal conductivity of liquid 7% GNP/RT-44 is lower than solid RT-44. The same negative effect was dominant due to the early formation of convective currents at a discharge rate of 6C. On the contrary, the macro/nano enhanced RT-44 is totally successful at keeping the battery cells below 45°C at all discharge rates.

The effective protection time is defined as the period it takes for the maximum temperature of the battery pack to exceed 45°C. Figure 9 shows the effective protection times and performance enhancement percentages of macro and/or nano enhanced RT-44 in comparison with RT-44 thermal protection. The effective protection times for the natural convection were measured as 933 s (2.7C), 354 s (4C), 223 s (5.1C) and 158 s (6C) from Figure 9. In all other thermal protection methods, completely effective protection was provided throughout the related discharge time for the discharge rate of 2.7C

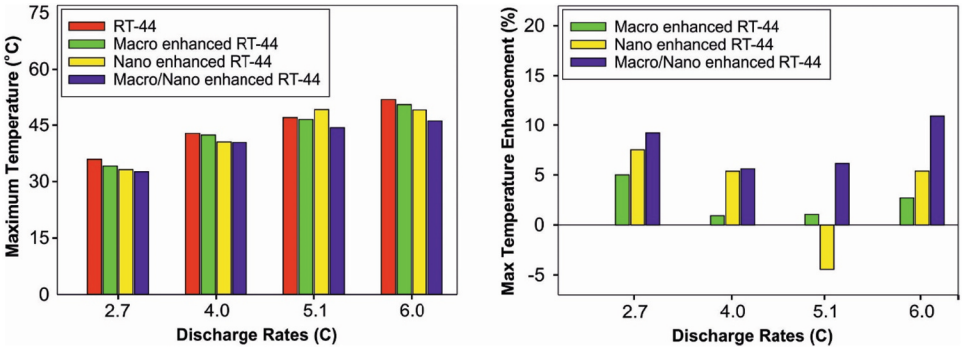

Figure 8. The maximum temperatures and the percent performance enhancements compared to RT-44.

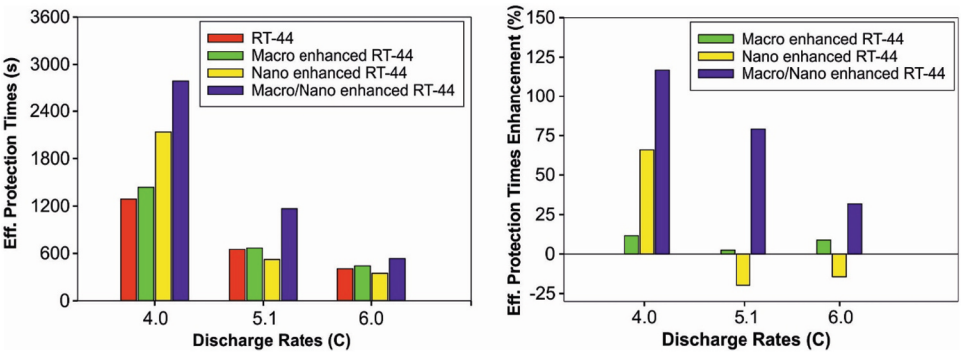

Figure 9. The effective protection times and percent performance enhancements compared to RT-44.

and 4C. Although it does not provide complete protection at high discharge rates (≥5.1C), significant improvements are achieved compared to the unprotected battery pack. Such that in the use of RT-44, effective protection times are increased by 2.9 (5.1C) and 2.6 (6C) times compared to natural convection cases. On the other hand, the enhanced RT-44 composites (except nano one), improve the battery protection performances by further prolonging the effective protection times. The macro/nano enhanced RT-44 provides the best performances in terms of effective protection times. It improves the effective protection times by 117% (4C), 79% (5.1C) and 32% (6C) compared to RT-44.

Another performance criterion is to keep the maximum temperature difference throughout the battery pack below 5°C. The maximum temperature difference of the battery pack can be defined as the difference between the measurement point of $\#T_2$ in the interior and $\#T_1$ in the outer region. Figure 10 shows the maximum temperature difference-time variation throughout the battery pack with different thermal

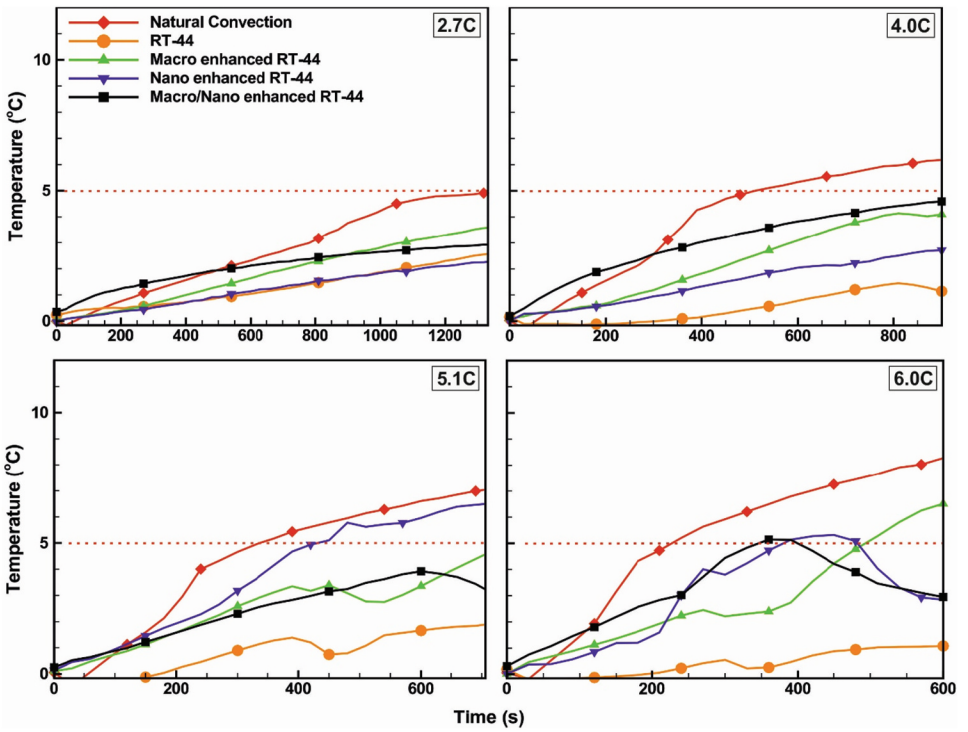

Figure 10. The maximum temperature difference-time variation throughout the battery pack.

protection methods. In natural convection, the maximum temperature differences throughout the battery pack exceeding 5°C (except for 2.7C) during the discharge process supports the necessity of thermal protection. The RT-44 based thermal protection seems to be successful at maintaining the maximum temperature difference below 5°C at all discharge rates. With the RT-44, the maximum temperature differences continuously increase until melting begins. The initiation of melting in the inner region of the package before the outer region reduces the maximum temperature difference and keeps it relatively small. In other words, continuity of the temperature ramp rate of $\#T_2$ and decrease of temperature ramp rate of $\#T_1$ causes a significant restriction in maximum temperature difference. On the other hand, nano and/or macro enhancement cause negligible performance loss in terms of maximum temperature difference only at a portion of high discharge rate of 5.1C and 6C. This is caused by the more efficient transfer of heat to the outer part of the pack as a result of enhanced thermal conductivity.

Similarly, giving consideration to battery pack thermal protection, the temperature difference throughout the cell height should be below 5°C. It was calculated as the difference between the temperature measured at the upper point ($\#T_6$) and the temperature measured at the lower point ($\#T_4$) of the cell. The temperature difference throughout the cell height was found to increase in proportion to the discharge rate. Figure 11 shows the temperature difference throughout the cell height with different thermal protection methods used at a discharge rate of 6.0C. In the case of natural convection, the mentioned temperature difference increases rapidly under the effect of buoyancy driven flow and exceeds 5°C toward the end of the discharge process. The buoyancy flow effects also apply to the liquid RT-44, but the temperature difference is significantly reduced due to its slow motion compared to natural convection. As a result, each thermal protection method provides a more uniform temperature distribution throughout the cell. In these cases, the maximum temperature differences throughout the cell were kept below 1°C. One of the reasons for a more uniform temperature distribution throughout the cell is the insufficient liquid fraction formed at the end of the discharge. Another reason is the suppression of buoyancy flows due to the macro and nano addition increasing the viscosity in the liquid phase.

The cooling times of PCM-based passive thermal protection systems are critical for reuse when the battery pack is off. Figure 12 compares the cooling performances of RT-44, macro and/or nano enhanced RT-44 thermal protections until the maximum temperature of the battery ($\#T_2$) drops below 30°C after 5.1C discharge. Macro enhancement of RT-44 is seen to be more effective than nano enhancement of RT-44 in terms of shortening the cooling time. The cooling times were measured as 9746, 7345 and 8858 seconds for RT-44, macro enhanced RT-44 and nano enhanced RT-44, respectively. In other words, the macro or nano enhanced RT-44 have 25% and 9% enhancement in cooling performance compared to the RT-44, respectively. The cooling time was determined as 6698 seconds in the macro/nano enhanced RT-44, and the macro enhancement can be said to have made a major contribution to the 31% performance enhancement.

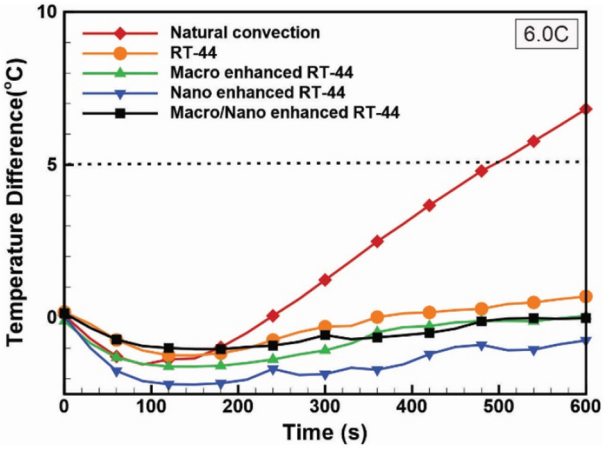

Figure 11. The temperature differences along the cell height.

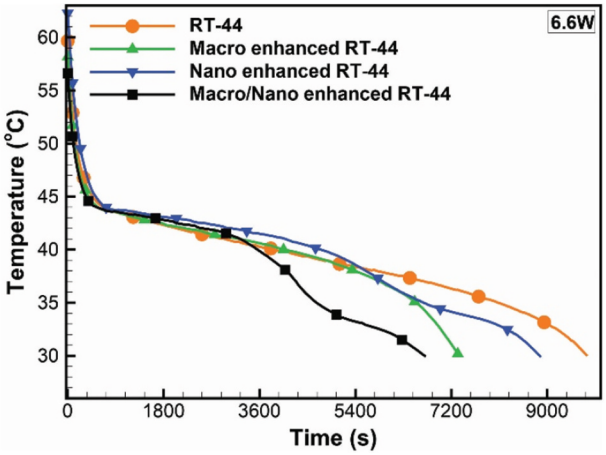

Figure 12. The cooling responses of the battery pack during the off time.

The continuous on/off cycles of the battery pack was performed to examine the heat accumulation effect on the subsequent operations. As shown in Figure 13, all thermal protection methods have been tested in a five-cycle scenario where the representative battery pack was operated for 10 minutes and then stopped for 10 minutes for each cycle. Since the heat accumulated in the battery pack is not completely dissipated to the environment, the maximum temperature continuously rises as a result of the subsequent discharge processes. In the unprotected (natural convection) battery pack, the maximum temperature approaches 100°C in the 5^{th} cycle. With the RT-44, the maximum temperature of the battery pack was determined as 56°C in 5^{th} cycle. However, it is clear that the thermally enhanced RT-44 provides better performance due to slower temperature rise during discharge and faster temperature drop during battery pack is not operated. The positive effect of macro enhancement on cooling performance keeps the maximum temperature in the 5th cycle 2.4°C and 4.4°C lower for RT-44 and 7% GNP/RT-44, respectively. Especially for the Macro/Nano enhanced RT-44, the maximum temperature at the end of the charge/discharge cycles could be reduced to an acceptable temperature of 47.5°C. However, for all enhancement methods, temperature is over 45°C from the 3rd cycle. When the on/off cycles are compared in terms of the maximum temperature difference, the nano enhancement provides good protection up to the 4th cycle. Macro/nano enhancement, on the other hand, keeps the maximum temperature difference below 5°C throughout the whole cycle.

As a result, nano and macro enhanced thermal conductivity will improve the battery pack's ability to radiate outward heat accumulated in its interior. If this capability is combined with an arrangement such as passing air around the battery pack while the electric vehicle is in motion, it can become a practically usable system with a completely efficient thermal protection.

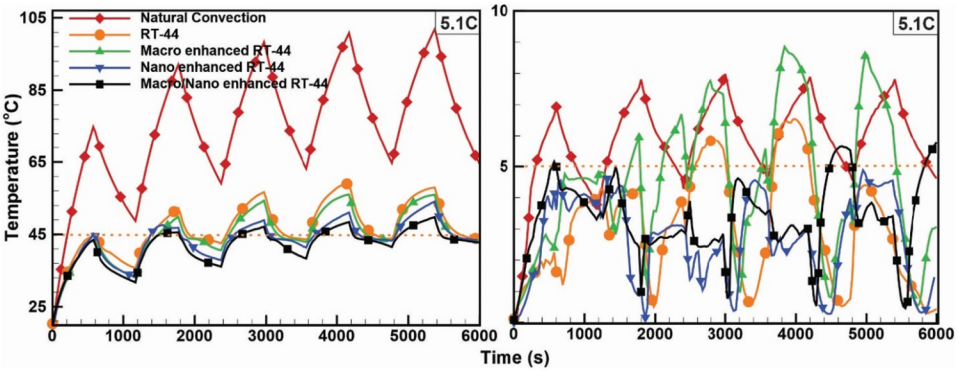

Figure 13. On/off cycles.

Table 3. Summary of results for different PCM-based thermal protection methods.

Thermal Protection Method	Maximum Temp. (°C)				Maximum Temp. Difference (°C)			
	2.7C	4.0C	5.1C	6.0C	2.7C	4.0C	5.1C	6.0C
RT-44	35.9	42.8	47.2	52.1	2.6	1.5	1.9	2.9
Macro enhanced RT-44	34.2	42.5	46.7	50.6	3.6	4.1	4.6	6.5
Nano enhanced RT-44	33.2	40.5	49.3	49.3	2.3	2.7	6.5	5.3
Macro/Nano enhanced RT-44	32.6	40.4	44.3	46.3	2.9	4.5	3.9	5.1

A summary of the results for the RT-44, macro enhanced RT-44, nano enhanced RT-44, and makro/nano enhanced RT-44 are given in Table 3.

4. Conclusions

In the present study, the thermal protection performances of macro and/or nano enhanced organic PCM were tested from low to high discharge rates in a representative battery pack. Thermal protection performances were compared according to keeping the maximum temperature below 45°C and the maximum temperature difference below 5°C, and the following conclusions were drawn.

- The positive effect of macro enhancement on thermal conductivity increase is 1.97 times and nano enhancement is 3.3 times. The coupled effect of the macro and nano enhancement in thermal conductivity increase is 4.2 times relative to only the PCM case.
- Macro and/or nano enhancements create a thermal protection advantage by reducing the constant temperature plateau to a lower temperature.
- At discharge rates of 2.7C and 4.0C, all PCM-based thermal protection methods keep the maximum battery pack temperature below 45°C. Conversely, at relatively high discharge rates of 5.1C and 6.0C, the macro/nano enhanced PCM performs best at limiting the maximum temperature.
- The pure PCM is quite successful at keeping the maximum temperature difference below 5°C. Although macro or nano enhancement deteriorates the performance in this respect, it can be accepted that the macro/nano enhanced PCM keeps the maximum temperature difference below 5°C.
- The macro/nano enhanced RT-44 enhances the effective protection times compared to RT-44 by 117%, 79% and 32% at 4C, 5.1C and 6.0C respectively.
- Macro/nano enhancement significantly shortens the cooling time of the heat accumulated RT-44. In fact, macro enhancement greatly contributes to the cooling time performance.
- Macro/Nano enhanced RT-44 maintains the maximum temperature and maximum temperature difference within the allowable limit due to the slower temperature rise during discharge and the faster temperature drop during cooling operation.

Another method of reducing the PCM thermal temperature plateau seems to be lowering the PCM melting temperature. The next study is planned to examine the effects of lowering the PCM melting temperature as much as possible in order to take advantage of phase change. At the same time, the variation of the heat emitted by the battery cells with time will be tested using a variable current to consider the state of charge effect.

Nomenclature

T	temperature (°C)	m	melting
k	thermal conductivity (W/mK)		
H	latent heat (J/g)		**Acronyms**
μ	dynamic viscosity (kg/ms)	PCM	Phase Change Material
		GNP	Graphene Nanoplatelets
	Subscripts	EG	Expanded Graphite
om	onset melting	DSC	Differential Scanning Calorimetry
em	endset melting	S	Stage
max	maximum		

Disclosure statement

No potential conflict of interest was reported by the author(s).

Funding

This work was supported by the Sivas Cumhuriyet University Scientific Research Projects Commission (CUBAP), Turkey [M-622].

ORCID

Umit Nazli Temel http://orcid.org/0000-0001-5053-5124
Ferhat Kilinc http://orcid.org/0000-0003-2707-6438

References

[1] A. Jarrett and I. Y. Kim, "Design optimization of electric vehicle battery cooling plates for thermal performance," *J. Power Sources*, vol. 196, no. 23, pp. 10359–10368, 2011. DOI: 10.1016/j.jpowsour.2011.06.090.
[2] C. Lin, S. Xu, G. Chang, and J. Liu, "Experiment and simulation of a LiFePO4 battery pack with a passive thermal management system using composite phase change material and graphite sheets," *J. Power Sources*, vol. 275, pp. 742–749, 2015. DOI:10.1016/j.jpowsour.2014.11.068.
[3] E. Gümüşsu, Ö. Ekici, and M. Köksal, "3-D CFD modeling and experimental testing of thermal behavior of a Li-Ion battery," *Appl. Therm. Eng*, vol. 120, pp. 484–495, 2017. DOI:10.1016/j.applthermaleng.2017.04.017.
[4] Y. S. Ranjbaran, S. J. Haghparast, M. H. S. G. R. Molaeimanesh, and G. R. Molaeimanesh, "Numerical evaluation of a thermal management system consisting PCM and porous metal foam for Li - ion batteries," *J. Therm. Anal. Calorim*, vol. 141, no. 5, pp. 1717–1739, 2020. DOI: 10.1007/s10973-019-08989-w.
[5] H. Yang, H. Zhang, Y. Sui, and C. Yang, "Numerical analysis and experimental visualization of phase change material melting process for thermal management of cylindrical power battery," *Appl. Therm. Eng*, vol. 128, pp. 489–499, 2018. DOI:10.1016/j.applthermaleng.2017.09.022.
[6] P. Ramadass, B. Haran, R. White, and B. N. Popov, "Capacity fade of Sony 18650 cells cycled at elevated temperatures: part I. Cycling performance," *J. Power Sources*, vol. 112, no. 2, pp. 606–613, 2002. DOI: 10.1016/S0378-7753(02)00474-3.
[7] A. A. Pesaran, "Battery thermal models for hybrid vehicle simulations," *Journal of Power Sources*, vol. 110, no. 2, pp.377–382, 2002. DOI: 10.1016/S0378-7753(02)00200-8.
[8] J. P. Hadiya and A. K. N. Shukla, "Experimental thermal behavior response of paraffin wax as storage unit," *J. Therm. Anal. Calorim*, vol. 124, no. 3, pp. 1511–1518, 2016. DOI: 10.1007/s10973-016-5276-2.
[9] N. O. Moraga, J. P. Xamán, and R. H. Araya, "Cooling Li-ion batteries of racing solar car by using multiple phase change materials," *Appl. Therm. Eng*, vol. 108, pp. 1041–1054, 2016. DOI:10.1016/j.applthermaleng.2016.07.183.
[10] J. Yan, Q. Wang, K. Li, and J. Sun, "Numerical study on the thermal performance of a composite board in battery thermal management system," *Appl. Therm. Eng*, vol. 106, pp. 131–140, 2016. DOI:10.1016/j.applthermaleng.2016.05.187.
[11] J. Chen, *et al.*, "Effects of different phase change material thermal management strategies on the cooling performance of the power lithium ion batteries: a review," *J. Power Sources*, vol. 442, no. September, pp. 227228, 2019. DOI: 10.1016/j.jpowsour.2019.227228.
[12] W. Ye, "Enhanced latent heat thermal energy storage in the double tubes using fins," *J. Therm. Anal. Calorim*, 2016. DOI: 10.1007/s10973-016-5870-3.
[13] F. Bahiraei, A. Fartaj, and G. A. Nazri, "Experimental and numerical investigation on the performance of carbon-based nanoenhanced phase change materials for thermal management applications," *Energy Convers. Manag*, vol. 153, pp. 115–128, 2017. DOI:10.1016/j.enconman.2017.09.065.
[14] S. A. Khateeb, M. M. Farid, J. R. Selman, and S. Al-Hallaj, "Design and simulation of a lithium-ion battery with a phase change material thermal management system for an electric scooter," *J. Power Sources*, vol. 128, no. 2, pp. 292–307, 2004. DOI: 10.1016/j.jpowsour.2003.09.070.
[15] P. Ping, R. Peng, D. Kong, G. Chen, and J. Wen, "Investigation on thermal management performance of PCM-fin structure for Li-ion battery module in high-temperature environment," *Energy Convers. Manag*, vol. 176, no. August, pp. 131–146, 2018. DOI: 10.1016/j.enconman.2018.09.025.
[16] Z. Wang, H. Zhang, and X. Xia, "Experimental investigation on the thermal behavior of cylindrical battery with composite paraffin and fin structure," *Int. J. Heat Mass Transf*, vol. 109, pp. 958–970, 2017. DOI:10.1016/j.ijheatmasstransfer.2017.02.057.

[17] S. A. Khateeb, S. Amiruddin, M. Farid, J. R. Selman, and S. Al-Hallaj, "Thermal management of Li-ion battery with phase change material for electric scooters: experimental validation," *J. Power Sources*, vol. 142, no. 1–2, pp. 345–353, 2005. DOI: 10.1016/j.jpowsour.2004.09.033.

[18] R. Kizilel, *et al*., "Passive control of temperature excursion and uniformity in high-energy Li-ion battery packs at high current and ambient temperature," *J. Power Sources*, vol. 183, no. 1, pp. 370–375, 2008. DOI: 10.1016/j.jpowsour.2008.04.050.

[19] W. Q. Li, Z. G. Qu, Y. L. He, and Y. B. Tao, "Experimental study of a passive thermal management system for high-powered lithium ion batteries using porous metal foam saturated with phase change materials," *J. Power Sources*, vol. 248, 2014. DOI: 10.1016/j.jpowsour.2014.01.006.

[20] Z. Rao, Y. Huo, X. Liu, and G. Zhang, "Experimental investigation of battery thermal management system for electric vehicle based on paraffin/copper foam," *J. Energy Inst*, vol. 88, no. 3, pp. 241–246, 2015. DOI: 10.1016/j.joei.2014.09.006.

[21] A. Mills and S. Al-Hallaj, "Simulation of passive thermal management system for lithium-ion battery packs," *J. Power Sources*, vol. 141, no. 2, pp. 307–315, 2005. DOI: 10.1016/j.jpowsour.2004.09.025.

[22] R. Zhao, J. Gu, and J. Liu, "Optimization of a phase change material based internal cooling system for cylindrical Li-ion battery pack and a hybrid cooling design," *Energy*, vol. 135, pp. 811–822, 2017. DOI:10.1016/j.energy.2017.06.168.

[23] T. Xu, *et al*., "Experimental and numerical investigation of the application of phase change materials in a simulative power batteries thermal management system," *Appl. Energy*, vol. 121, pp. 104–113, 2014. DOI: 10.1016/j.apenergy.2014.01.075.

[24] G. Jiang, J. Huang, M. Liu, and M. Cao, "Experiment and simulation of thermal management for a tube-shell Li-ion battery pack with composite phase change material," *Appl. Therm. Eng*, vol. 120, pp. 1–9, 2017. DOI:10.1016/j.applthermaleng.2017.03.107.

[25] U. N. Temel, S. Kurtulus, M. Parlak, and K. Yapici, "Size-dependent thermal properties of multi-walled carbon nanotubes embedded in phase change materials," *J. Therm. Anal. Calorim*, vol. 132, no. 1, pp. 631–641, 2018. DOI: 10.1007/s10973-018-6966-8.

[26] L. W. Fan, *et al*., "Effects of various carbon nanofillers on the thermal conductivity and energy storage properties of paraffin-based nanocomposite phase change materials," *Appl. Energy*, vol. 110, pp. 163–172, 2013. DOI: 10.1016/j.apenergy.2013.04.043.

[27] A. Babapoor, M. Azizi, and G. Karimi, "Thermal management of a Li-ion battery using carbon fiber-PCM composites," *Appl. Therm. Eng*, vol. 82, pp. 281–290, 2015. DOI:10.1016/j.applthermaleng.2015.02.068.

[28] X. Tong, *et al*., "The effects of various carbon nanofillers on the thermal properties of paraffin for energy storage applications," *J. Therm. Anal. Calorim*, vol. 124, no. 1, pp. 181–188, 2015. DOI: 10.1007/s10973-015-5153-4.

[29] U. N. Temel, K. Somek, M. Parlak, and K. Yapici, "Transient thermal response of phase change material embedded with graphene nanoplatelets in an energy storage unit," *J. Therm. Anal. Calorim*, vol. 133, no. 2, pp. 907–918, 2018. DOI: 10.1007/s10973-018-7161-7.

[30] P. Goli, *et al*., "Graphene-enhanced hybrid phase change materials for thermal management of Li-ion batteries," *J. Power Sources*, vol. 248, pp. 37–43, 2014. DOI:10.1016/j.jpowsour.2013.08.135.

[31] U. N. Temel, "Passive thermal management of a simulated battery pack at different climate conditions," *Appl. Therm. Eng*, vol. 158, no. May, pp. 113796, 2019. DOI: 10.1016/j.applthermaleng.2019.113796.

[32] Z. Ling, F. Wang, X. Fang, X. Gao, and Z. Zhang, "A hybrid thermal management system for lithium ion batteries combining phase change materials with forced-air cooling," *Appl. Energy*, vol. 148, pp. 403–409, 2015. DOI:10.1016/j.apenergy.2015.03.080.

[33] D. Kong, *et al*. "A novel battery thermal management system coupling with PCM and optimized controllable liquid cooling for different ambient temperatures". *Energy Convers. Manag*, Vol. 204, no. November, pp. 112280, 2019, 2020. DOI: 10.1016/j.enconman.2019.112280.

[34] Y. Lv, *et al*., "Experimental study on a novel battery thermal management technology based on low density polyethylene-enhanced composite phase change materials coupled with low fins," *Appl. Energy*, vol. 178, pp. 376–382, 2016. DOI:10.1016/j.apenergy.2016.06.058.

[35] C. V. Hémery, F. Pra, J. F. Robin, and P. Marty, "Experimental performances of a battery thermal management system using a phase change material," *J. Power Sources*, vol. 270, pp. 349–358, 2014. DOI:10.1016/j.jpowsour.2014.07.147.